AtABCG29 is a monolignol transporter involved in lignin biosynthesis

Alejandro, Santiago ; Lee, Yuree ; Tohge, Takayuki ; Sudre, Damien ; Osorio, Sonia ; Park, Jiyoung ; Bovet, Lucien ; Lee, Youngsook ; Geldner, Niko ; Fernie, Alisdair R ; Martinoia, Enrico

Abstract: Lignin is the defining constituent of wood and the second most abundant natural polymer on earth. Lignin is produced by the oxidative coupling of three monolignols: p-coumaryl alcohol, coniferyl alcohol, and sinapyl alcohol. Monolignols are synthesized via the phenylpropanoid pathway and eventually polymerized in the cell wall by peroxidases and laccases. However, the mechanism whereby monolignols are transported from the cytosol to the cell wall has remained elusive. Here we report the discovery that AtABCG29, an ATP-binding cassette transporter, acts as a p-coumaryl alcohol transporter. Expression of AtABCG29 promoter-driven reporter genes and a Citrine-AtABCG29 fusion construct revealed that AtABCG29 is targeted to the plasma membrane of the root endodermis and vascular tissue. Moreover, yeasts expressing AtABCG29 exhibited an increased tolerance to p-coumaryl alcohol by excreting this monolignol. Vesicles isolated from yeasts expressing AtABCG29 exhibited a p-coumaryl alcohol transport activity. Loss-of-function Arabidopsis mutants contained less lignin subunits and were more sensitive to p-coumaryl alcohol. Changes in secondary metabolite profiles in abcg29 underline the importance of regulating p-coumaryl alcohol levels in the cytosol. This is the first identification of a monolignol transporter, closing a crucial gap in our understanding of lignin biosynthesis, which could open new directions for lignin engineering.

DOI: https://doi.org/10.1016/j.cub.2012.04.064

Title

AtABCG29 is a monolignol transporter involved in lignin biosynthesis

Authors / Affiliations

Santiago Alejandro[1*‡], Yuree Lee[2*], Takayuki Tohge[3*], Damien Sudre[1*†], Sonia Osorio[3], Jiyoung Park[4], Lucien Bovet[1,5], Youngsook Lee[4], Niko Geldner[2], Alisdair R. Fernie[3] and Enrico Martinoia[1]

[1]Institut für Pflanzenbiologie, Universität Zürich, 8008 Zurich, Switzerland

[2]Department of Plant Molecular Biology, University of Lausanne, Quartier Sorge, Lausanne, 1015, Switzerland

[3]Max-Planck-Institute of Molecular Plant Physiology, Am Muehlenberg 1. Potsdam, 14476, Germany

[4]POSTECH-UZH Cooperative Laboratory, Department of Integrative Bioscience and Biotechnology, Pohang University of Science and Technology, Pohang 790-784, Korea

[5]Current address: Philip Morris Products S.A., PMI R&D, Neuchâtel, Switzerland

[†]Current Address: Biochimie et Physiologie Moleculaire des Plantes, Centre National de la Recherche Scientifique, Institut National de la Recherche Agronomique, Université Montpellier 2, SupAgro. Bat 7, 2 place Viala, 34060 Montpellier cedex 1, France

*These authors contributed equally to the work described in this manuscript

[‡]Corresponding authors: Santiago Alejandro e-mail: saalmar333@hotmail.com

Takayuki Tohge e-mail: Tohge@mpimp-golm.mpg.de

Summary

Lignin is the defining constituent of wood and the second most abundant natural polymer on earth. Lignin is produced by the oxidative coupling of three monolignols, *p*-coumaryl alcohol, coniferyl alcohol and sinapyl alcohol [1]. Monolignols are synthesized via the phenylpropanoid pathway and eventually polymerized in the cell wall by peroxidases and laccases. However, the mechanism whereby monolignols are transported from the cytosol to the cell wall has remained elusive. Here we report the discovery that AtABCG29, an ATP-binding cassette transporter, acts as a *p*-coumaryl alcohol transporter. Expression of *AtABCG29* promoter driven-reporter genes and a *citrine-AtABCG29* fusion construct revealed that AtABCG29 is targeted to the plasma membrane of the root endodermis and vascular tissue. Moreover, yeasts expressing AtABCG29 exhibited an increased tolerance to *p*-coumaryl alcohol by excreting this monolignol. Vesicles isolated from yeasts expressing AtABCG29 exhibited a *p*-coumaryl alcohol transport activity. Loss-of-function Arabidopsis mutants contained less lignin subunits and were more sensitive to *p*-coumaryl alcohol. Changes in secondary metabolites profiles in *abcg29* underline the importance of regulating *p*-coumaryl alcohol levels in the cytosol. This is the first identification of a monolignol transporter, closing a crucial gap in our understanding of lignin biosynthesis, which could open new directions for lignin engineering.

Highlights

ABC transporters, monolignol transport, lignin biosynthesis, endodermis

Results and Discussion

Coexpression analysis of AtABCG29

Lignin is an important component of cell walls that gives structural rigidity to plants. Identification of lignin biosynthetic genes has attracted much attention during the last decade. All steps of the phenylpropanoid biosynthesis leading to lignin precursors are carried out within the plant cell [2]. However, the last step, polymerization of the monolignols occurs in the apoplastic space. This requires that monolignols are transported across the plasma membrane, a process that has been recently reported to be an ATP hydrolysis-dependent transport [3]. In order to identify genes involved in monolignol transport, we performed a coexpression network analysis with the ABCG-transporter subfamily (previously called WBCs and PDRs) of Arabidopsis using the ATTED-II database (http://atted.jp/). Members of the ABCG subfamily have been shown to transport a broad range of fatty acids and terpenoids. We therefore wondered whether this class could also be implicated in the transport of phenolic compounds. The results revealed that AtABCG29/PDR1, a member of the full size ABCG subfamily [4,5], exhibited a high coexpression ratio with three genes of the phenylpropanoid biosynthesis pathway (Figure S1), which are involved in the synthesis of lignin and flavonoids [1]. The well-correlated genes correspond to two 4-coumarate coenzyme A ligases (4CL2 and 4CL5), which convert hydroxycinnamic acids into hydroxycinnamoyl CoA esters and one caffeoyl CoA-*O*-methyltransferase catalyzing the conversion of caffeoyl CoA into feruloyl CoA [6]. Moreover, seven further genes related to phenylpropanoid biosynthesis are coexpressed with AtABCG29, albeit with lower coexpression ratios (Figure S1). In concordance with our data, Ehlting and colleagues [7] reported that AtABCG29 showed an expression pattern, in primary stems, consistent with that of monolignol biosynthetic genes and

increased lignin content. Therefore, these results rendered AtABCG29 a good candidate transporter for monolignol export.

Tissue-specific expression and subcellular localization of AtABCG29

To investigate tissue-specific expression, a 2.2 kb fragment upstream the *AtABCG29* coding sequence was used to drive the expression of the GUS reporter. GUS activity was detected mainly in the primary and secondary roots, but not in the root tip (Figures 1A-C). Meristematic cells at the root tip do not deposit lignin, therefore the expression pattern observed in Figure 1B corresponds to that expected for a monolignol exporter [8]. In addition, in two-week-old plants no GUS signals were detected in the hypocotyl and the upper part of the primary root (Figure S2A), probably since in this part of the root monolignol synthesis and deposition is reduced [9,10]. We also detected GUS expression in the lower part of the stem and whole vasculature of rosette leaves (Figure S2B) and anthers, where the endothecium contains a high level of lignin and siliques (Figure S2C-D) [11]. Public microarray data indicates that AtABCG29 is expressed mainly in the roots and stems (http://bar.utoronto.ca/efp_arabidopsis/cgi-bin/efpWeb.cgi) corresponding to the parts of a plant containing a higher amount of lignin [12], while expression in flowers and siliques is lower. In order to get a higher resolution of the expression pattern, we fused the 2.2kb upstream fragment to the 42 kDa fluorescent reporter protein NLS-GFP that contains a classical nuclear localization sequence (NLS) but lacks nuclear retention or export signals [13]. This construct demonstrated that *AtABCG29* is only expressed in the endodermis and vascular tissue above the elongation zone (Figures 1D-F). These results are consistent with the Arabidopsis Gene Expression Database

(AREX) (www.arexdb.org) and further support the hypothesis that AtABCG29 might be involved in lignin biosynthesis.

To study the subcellular localization of AtABCG29, a yellow fluorescent protein (Citrine) was fused to the N-terminus of AtABCG29 (ABCG29N) and expressed under the control of an endodermis specific promoter (*pCASP1::Citrine-ABCG29N*) [14], and of the endogenous promoter (*pABCG29::Citrine-ABCG29N*). Endodermis-specific expression was chosen because the endodermis is the largest and outermost cell layer in which ABCG29 is endogenously expressed and *pCASP1* drives strong expression in this cell layer making it ideal for subcellular localization studies. Citrine-AtABCG29N was detected at the plasma membrane of the endodermis except in the Casparian strip domain (CSD) (Figures 1G-I). The *pABCG29::Citrine-ABCG29N* protein was also detected in the plasma membrane of endodermal cells (Figures 1J-K), albeit with a much weaker signal. The fact that the fluorescent signal is interrupted in the CSD, where plasma membrane proteins are excluded [15] indicates that the peripheral AtABCG29 signal represents indeed plasma membrane and not cortical ER or the vacuole, in which cases a continuous signal would be expected.

Functional analysis of the AtABCG29 gene product

The three most abundant monolignols are *p*-coumaryl alcohol, coniferyl alcohol, and sinapyl alcohol. Upon incorporation into the lignin polymer, these monomers are referred to as *p*-hydroxyphenyl (H), guaiacyl (G), and syringyl (S) units, respectively [1,2]. Since we hypothesized that AtABCG29 is involved in lignin synthesis acting as a monolignol exporter, we expressed AtABCG29 in the YMM12 yeast strain that

carries loss-of-function mutations in eight ABC transporters. The mutant displays delayed growth even under normal growth conditions (Figure 2A), which was expected since many of the PDRs are important for cellular detoxification and cell fitness during cell growth [16]. We therefore tested the effect of the three monolignols on yeast growth. The addition of coniferyl alcohol to the growth medium decreased the growth rates of YMM12 but also those of the wild type and YMM12 expressing ABCG29 (Figure S3A). No significant effect could be observed in the presence of sinapyl alcohol in any strain tested (Figure S3B). In contrast, while upon exposure to *p*-coumaryl alcohol, growth of the wild-type yeast was not affected, that of YMM12 was strongly retarded compared to that on control medium. YMM12 expressing AtABCG29 exhibited an intermediary phenotype, indicating that this ABCG protein was able to export *p*-coumaryl alcohol and reduce its toxic effect in yeast (Figure 2B). In order to gain further proof as to whether AtABCG29 acts as a *p*-coumaryl alcohol transporter, we performed time-dependent loading and unloading assays. Yeast expressing AtABCG29 accumulated less *p*-coumaryl alcohol than the empty vector control (Figure 2C). Our hypothesis could be confirmed by performing efflux analysis from preloaded yeasts. While *p*-coumaryl alcohol was only slowly released from YMM12 cells, both wild type and AtABCG29 expressing cells efficiently released *p*-coumaryl alcohol (Figure 2D). The transport of *p*-coumaryl alcohol by ABCG29 transporter appears to be substrate-specific because no differences were observed in loading and unloading analysis of sinapyl or coniferyl alcohol in yeast cells (data not shown). ABCG29 expressing yeasts export similar amounts of *p*-coumaryl alcohol to its corresponding wild type despite that it grows more slowly in the presence of this monolignol. This can be explained by the fact that growth of the multiple mutant is not only affected by *p*-coumaryl alcohol (Fig. 2A). Further evidence

that AtABCG29 acts as a *p*-coumaryl alcohol transporter was obtained by performing transport experiments with yeast microsomes. The efflux activity observed in yeast cells can be detected as *p*-coumaryl alcohol uptake after the addition of MgATP, because the membrane isolation results in a mixed population of right side-out and inside-out vesicles. The uptake of *p*-coumaryl alcohol into yeast vesicles was strongly increased in vesicles isolated from AtABCG29 expressing yeast (Figure 2E). The residual transport activity may be due to diffusion, or to an intrinsic low capacity transporter [17]. Furthermore, vanadate, which is an effective inhibitor of ABC transporters, inhibited the ATP-dependent *p*-coumaryl alcohol uptake to more than 60% while NH_4Cl, which abolishes the transmembrane H^+ gradients, exhibited a negligible inhibitory effect, (Figure 2F). To test whether ABCG29 could transport other components of lignin biosynthesis we performed further transport experiments with yeast microsomes. The uptake of sinapyl alcohol was slightly increased (Figure S3C) but no differences were observed for coniferyl alcohol, cinnamic acid, ferulic acid or caffeic acid (data not shown). These results strongly suggest that AtABCG29 represents a *p*-coumaryl alcohol exporter that may have some minor activity towards sinapyl alcohol.

Phenotype of *abcg29* mutant lines

To get further evidence that AtABCG29 acts also as a *p*-coumaryl alcohol exporter in planta, we tested whether *abcg29* knockout mutants are more sensitive to toxic concentrations of *p*-coumaryl alcohol. We identified two T-DNA insertion lines for *AtABCG29* in the SALK collection (SALK_081047; *abcg29-1* and SALK_102381; *abcg29-2)* (Figure 3A). Using these seeds, we isolated two homozygous loss-of-function mutants (Figure 3B). When plants were grown on *p*-coumaryl alcohol

supplemented medium, root lengths of the loss-of-function mutants were significantly shorter than those of the wild-type plants (Figure 3C-D). No significant growth difference could be observed on control MS agar plates. To determine whether AtABCG29 is involved in resistance to other components of lignin biosynthesis, *abcg29* loss-of-function mutant plants were grown on media containing sinapyl alcohol, coniferyl alcohol, cinnamic acid, ferulic acid or caffeic acid; however, the growth rates were not different from those of wild-type plants (data not shown). In plants ABCGs are very often upregulated by their substrate. Therefore we performed a qRT-PCR analysis for *AtABCG29* RNA levels upon exposition of 5 mM *p*-coumaryl, sinapyl or coniferyl alcohol. While a 3.5 fold upregulation was observed for plants exposed to *p*-coumaryl alcohol after 8 hours (Fig 3E) no differences were detected for sinapyl or coniferyl alcohol (data not shown). These results further underline the importance of AtABCG29 in exporting *p*-coumaryl alcohol.

Differential accumulation of monolignols and non-targeted metabolite profiling

At this point, it was important to determine whether the absence of *AtABCG29* has an impact on lignin contents or monolignol composition. To answer this question, we used a targeted GC-MS metabolite profiling of thioacydolised roots [18,19]. Using this approach we succeeded to obtain highly reproducible results. Interestingly, not only the H content , but also G and S were significantly reduced in the *abcg29* knockout mutants by 23 and 32%, respectively (Table I). In wild type as well as in mutant plants guaiacyl (G) was the by far predominant constituent, while low levels of both *p*-hydroxyphenyl (H), and siringyl (S) units, constitute only approximately 8 and 5%, respectively of the total lignin (Table I). These data are not in concordance with the accepted idea that lignin of angiosperms consists mainly of G and S units and a low

content of H subunit [2]. Based on the transport specificity of AtABCG29 for H (Figure 2,3), we could hypothesize that altered export of *p*-coumaryl alcohol can affect biosynthesis and/or transport of coniferyl and sinapyl alcohol, thus resulting in an overall effect on lignin synthesis. The fact that despite a reduction in lignin contents we could not observe a phenotype is not surprising, since it was shown that plants with less lignin, changes in the H/G/S proportion or with the presence of other phenolic compounds in the lignin composition show little or no obvious phenotypic effects [2,20,21]. The observation that the amount of G and S, monolignols which are not or only marginally transported by ABCG29 are decreased, raised the question, whether also other metabolites where affected in this mutant. To answer this question we performed unbiased metabolite analyses using GC-MS and LC-MS. Interestingly, the levels of flavonols and aliphatic glucosinolates in the *abcg29* mutant lines are much lower than in the wt (Figure S4A). In a more detailed experiment, the lower part of plantlets was divided into three parts: root tip, main root and hypocotyls and the resulting sections were analyzed separately. In the root tip and hypocotyls, only slight changes in flavonols and glucosinolates contents were observed when compared to the wild type By contrast, we observed a strong decrease of these metabolites in the mid part (Figure S4B). The changes in the flavonol and glucosinolates profiles are well-correlated with the expression of ABCG29 in roots (Figure 1). When assessed at the individual metabolite level, *abcg29-1* and *abcg29-2* had reduced levels in the roots of quercetin (Q) and kaempferol (K) derived flavonoids [22], anthocyanin 9 (A9), sinapoyl-malate and sinapoyl-glucose [23], and 5 aliphatic and 3 indole glucosinolates [24]. In contrast, only minor changes could be observed for primary metabolites and most of these changes were not conserved across both mutants. To verify whether AtABCG29 could also act as a flavonoid

transporter we performed experiment with kaempferol and kaempferol-3-*O*-glucoside but could not detect any transport activity for these substrates (not shown). Interestingly, affecting glucosinolate biosynthesis has been shown to result in an altered pattern of phenylpropanoids [25].The metabolite profiling results suggest that decreased transport activity of p-coumaryl alcohol in the absence of AtABCG29 can regulate levels of diverse secondary metabolites in direct and indirect way. To gain more evidence for this hypothesis, qRT-PCR analysis for several genes coding for enzymes of the pathways where altered metabolite levels were observed, revealed that phenylammonia lyase (PAL1), chalcone synthase (CHS) and anthranilate synthase (ASB1), key enzymes for the production of phenolic compounds, flavonoids and glucosinolates, respectively, were consistently decreased (Figure S4C).

In summary, our experiments using yeast and plants strongly suggest that AtABCG29 is a *p*-coumaryl alcohol exporter. It may also play a minor role for sinapyl alcohol export. Analysis of the lignin constituents showed that in *abcg29* mutants not only p-hydroxyphenyl is present at lower amounts but also guaiacol and syringyl as well as a large number of flavonoids and glucosinolates. qRT-PCR analysis indicates that impaired export of *p*-coumaryl alcohol has a large impact on the complete metabolic pathway of phenolics and glucosinolates and hence, that the network and cross-talk of this metabolic network may be even more complex than assumed [26,27]. Nevertheless, identification of ABCG29 as a *p*-coumaryl transporter adds a new layer to our understanding of lignin biosynthesis and together with the discovery of additional monolignol tranporters could represent an important entry point for future manipulations of this pathway.

Experimental Procedures

See Supplemental Experimental Procedures

Acknowledgements: This work has been supported by the Spanish Ministry of Science and Innovation (MICINN) (SA), a grant of the SBF the within the COST action 859 (EM), The Swiss National Foundation (EM), Global Research Laboratory program of the Ministry of Education, Science and Technology of Korea Grant K20607000006 (to Y.L. and E.M.) and the Max-Planck-Society (TT and ARF).

References

1. Boerjan, W., Ralph, J., and Baucher, M. (2003). Lignin biosynthesis. Annu Rev Plant Biol 54, 519-546.
2. Bonawitz, ND., Chapple, C. (2010). The genetics of lignin biosynthesis: connecting genotype to phenotype. Annu Rev Genet. 44 337-363.
3. Miao, YC., Liu, CJ. (2010) ATP-binding cassette-like transporters are involved in the transport of lignin precursors across plasma and vacuolar membranes. Proc Natl Acad Sci 107 (52) 22728-22733.
4. Verrier, PJ., *et al* (2008). Plant ABC proteins--a unified nomenclature and updated inventory. Trends Plant Sci. 13(4) 151-159.
5. van de Brûle, S., and Smart, CC. (2002). The plant PDR family of ABC transporters. Planta 216 (1) 95-106.
6. Davin, LB., Jourdes, M., Patten, AM., Kim, KW., Vassão, DG., and Lewis, NG. (2008) Dissection of lignin macromolecular configuration and assembly:

comparison to related biochemical processes in allyl/propenyl phenol and lignan biosynthesis. Nat Prod Rep. 25 (6), 1015-90.

7. Ehlting, J., *et al*. (2005). Global transcript profiling of primary stems from Arabidopsis thaliana identifies candidate genes for missing links in lignin biosynthesis and transcriptional regulators of fiber differentiation. Plant J. 42 (5) 618-40.
8. Rogers, LA,. Campbell, MM. (2003). The genetic control of lignin deposition during plant growth and development. New Phytol. 164 (1) 17-30.
9. Benfey, PN., Schiefelbein, JW. (1994). Getting to the root of plant development: the genetics of Arabidopsis root formation. Trends Genet. 10 (3) 84-88.
10. Dolan, L., Roberts, K. (1995). Plant development: Pulled up by the roots. Curr Opin Genet Dev. 5 (4) 432-438.
11. Yang, C., Xu, Z., Song, J., Conner, K., Vizcay Barrena, G., Wilson, ZA. (2007) Arabidopsis MYB26/MALE STERILE35 regulates secondary thickening in the endothecium and is essential for anther dehiscence. Plant Cell. 19 (2) 534-548.
12. Goujon, T., Sibout, R., Eudes, A., MacKay, J., Jouanin, L. (2003). Genes involved in the biosynthesis of lignin precursors in *Arabidopsis thaliana*. Plant Physiol Biochem. 41 (8) 677-687.
13. Stochaj, U., Rassadi, R., Chiu, J. (2000) Stress-mediated inhibition of the classical nuclear protein import pathway and nuclear accumulation of the small GTPase Gsp1p. FASEB J. 14 (14) 2130-2132.
14. Roppolo, D., De Rybel, B., Tendon, VD., Pfister, A., Alassimone, J., Vermeer, JE., Yamazaki, M., Stierhof, YD., Beeckman, T., Geldner, N. (2011) A novel protein family mediates Casparian strip formation in the endodermis. Nature. 473 (7347) 380-3.

15. Alassimone, J., Naseer, S., Geldner, N. (2010) A developmental framework for endodermal differentiation and polarity. Proc Natl Acad Sci 107 (11) 5214-5219.
16. Jungwirth, H., Kuchler, K. (2006). Yeast ABC transporters-- a tale of sex, stress, drugs and aging. FEBS Lett. 580 (4) 1131-1138.
17. Nagy, R., Grob, H., Weder, B., Green, P., Klein, M., Frelet-Barrand, A., Schjoerring, JK., Brearley, C., Martinoia, E. (2009). The Arabidopsis ATP-binding cassette protein AtMRP5/AtABCC5 is a high affinity inositol hexakisphosphate transporter involved in guard cell signaling and phytate storage. J Biol Chem. 284 (48) 33614-33622.
18. Lapierre, C., Pollet, B. and Rolando C. (1995) New insights into the molecular architecture of hardwood lights by chemial degradative methods. Res. Chem. Intermed 21, 397-412.
19. Lapierre, C., Pollet, B., Petit-Conil, M., Toval, G., Romero, J., Pilate, G., Leple ,JC., Boerjan, W., Ferret, V., De Nadai, V., Jouanin, L. (1999). Structural alterations of lignins in transgenic poplars with depressed cinnamyl alcohol dehydrogenase or caffeic acid *O*-methyltransferase activity have an opposite impact on the efficiency of industrial kraft pulping. Plant Physiol. 119, 153–164.
20. Liu, CJ., Miao, YC., Zhang, KW. (2011) Sequestration and transport of lignin monomeric precursors. Molecules. 16 (1) 710-727.
21. Vanholme, R., Morreel, K., Ralph, J., Boerjan, W. (2008) Lignin engineering. Curr Opin Plant Biol. 11 (3) 278-285.
22. Santelia, D., Henrichs, S., Vincenzetti, V., Sauer, M., Bigler, L., Klein, M., Bailly, A., Lee, Y., Friml, J., Geisler, M., Martinoia, E. (2008) Flavonoids redirect PIN-mediated polar auxin fluxes during root gravitropic responses. J Biol Chem. 283 (45) 31218-31226.

23. Hause, B., Meyer, K., Viitanen, PV., Chapple, C., Strack, D. (2002) Immunolocalization of 1- O-sinapoylglucose:malate sinapoyltransferase in Arabidopsis thaliana. Planta. 215 (1) 26-32.
24. Petersen, BL., Chen, S., Hansen, CH., Olsen, CE., Halkier, BA. (2002) Composition and content of glucosinolates in developing Arabidopsis thaliana. Planta. 214 (4) 562-571.
25. Hemm, MR., Ruegger, MO., Chapple, C. (2003) The Arabidopsis *ref2* mutant is defective in the gene encoding CYP83A1 and shows both phenylpropanoid and glucosinolate phenotypes. Plant Cell. 15 (1) 179-194.
26. Yan, X., Chen, S. (2007) Regulation of plant glucosinolate metabolism. Planta. 226 (6) 1343-1352.
27. Besseau, S., Hoffmann, L., Geoffroy, P., Lapierre, C., Pollet, B., Legrand, M. (2007) Flavonoid accumulation in Arabidopsis repressed in lignin synthesis affects auxin transport and plant growth. Plant Cell. 19 (1) 148-162.

FIGURE 1. AtABCG29 is detected in vascular tissue and plasma membrane of endodermal cells in roots. *AtABCG29* promoter-GUS (*promABCG29::NLS-GFP-GUS*) reporter gene expression in 5-day-old seedling (**A**) and in 2-week-old plant root (**B**) and (**C**). For tissue localization of AtABCG29 was used a fluorescent reporter protein NLS-GFP driven by the native promoter (*promABCG29::NLS-GFP-GUS*). 5-day-old root seedling treated with 10 μM propidium iodide (**D**), GFP fluorescence (**E**) and overlay (**F**). Localization of *Citrine-ABCG29* expression that is driven by a specific endodermis promoter CASP1 (*pCASP1::ABCG29N-Citrine*) in 5-day old root seedling (**G**), under bright field illumination (**H**) and close-up image of a endodermal cell (**I**). *AtABCG29* promoter::*Citrine-ABCG29* (*pABCG29::Citrine-ABCG29*) gene expression in root endodermal cells (**J**) and bright field illumination (**K**). The arrowhead indicates position of the CSD. Scale bar in panel C corresponds to 5 μm.

FIGURE 2. Growth inhibition by *p*-coumaryl alcohol of a yeast ABC transporter mutant is rescued by expression of AtABCG29 that mediates the efflux of *p*-coumaryl alcohol. The growth of the indicated wild type yeast (YPH449, wt), mutant strain with the empty pNEV vector (YMM12) and *AtABCG29* overexpression (YMM12 ABCG29) was monitored. The yeast cells were grown in SCD (**A**) or SCD + 3mM *p*-coumaryl alcohol (**B**). The growth curves are derived from the mean values of four independent cultures for each time point. The experiment was repeated three times with similar results. (**C**) *p*-coumaryl alcohol accumulation. Cells from wild type yeast (black triangles) mutant strain with the empty pNEV vector (white circles) and *AtABCG29* overexpression (black circles) were grown overnight in SCD, and 2 mM *p*-coumaryl alcohol was added at time zero. (**D**) *p*-coumaryl alcohol efflux. Cells from

the yeast strains described for panel A were loaded with 2 mM *p*-coumaryl alcohol for 1.5 h at 4°C, washed, and resuspended in *p*-coumaryl alcohol-free SCD medium at time zero. Data of panel B are presented as the percentage of *p*-coumaryl alcohol concentration at time zero. Actual values of this 100% were 5.6, 8.7 and 4.7 pmol *p*-coumaryl alcohol/ mg yeast cells by wt, YMM12 and YMM12 ABCG29, respectively. (**E**) Time-dependent *p*-coumaryl alcohol uptake into microsomes. For non-ATP-dependent uptake, the reaction mix lacked ATP. Open circle, pNEV -ATP; filled circle, pNEV +ATP; open triangle, *pNEV-AtABCG29* -ATP; filled triangle, *pNEV-AtABCG29* +ATP. (**F**) Inhibition of AtABCG29 transport. Control, without inhibitor; 1.5 mM vanadate and 5 mM NH_4Cl. Results are the mean values of three independent cultures for each time point. The experiments were repeated four times with similar results. ** p <0.01.

FIGURE 3. AtABCG29 confers resistance against toxicity effects of *p*-coumaryl alcohol and is upregulated by this substrate. (**A**) Positions of the insertion in the T-DNA of *atabcg29* **.** Filled boxes and open boxes represent the 3′-untranslated region, and exons of the gene, respectively. Insertions were at 5th exon. (**B**) *AtABCG29* transcript levels in wild type and mutant lines determined by semi-quantitative RT-PCR. Total RNA was extracted using Trizol reagent. cDNAs were synthesized using an RT-PCR kit (Promega; http://www.promega.com/) with the M-MLV Reverse Transcriptase. **(C**) Inhibition of plant growth by *p*-coumaryl alcohol. Plants were grown in half-strength Murashige and Skoog medium for 2 weeks under long day conditions (16:8) at 22ºC. Col-0, wt plants. (**D**) Primary root lengths of 2-weeks-old seedlings grown under on medium supplemented with 1,5 or 2 mM p-

coumaryl alcohol (n>15). (**E**) Transcript levels of *AtABCG29* in root seedlings treated with 5 mM *p*-coumaryl alcohol. RNA was extracted from roots of 2-week-old seedlings grown in liquid culture. Total RNA was extracted using Trizol reagent. cDNAs were synthesized using an RT-PCR kit (Promega; http://www.promega.com/) with the M-MLV Reverse Transcriptase. The transcripts levels were quantified by qRT-PCR. To amplify *AtABCG29* cDNA, PCR was performed using the following specific primers: 5'-TCCGAAATGGTGGATATGGTA-3' and 5'-TGCCAAAAGCAAACATAAACG-3'. *Tubuline* primers: 5'-CCTGATAACTTCGTCTTTGG-3' (F) and 5'-GTGAACTCCATCTCGTCCAT-3'.Results are the mean values of three independent cultures. The experiment was repeated three times with similar results. * p <0.05 ** p<0.01

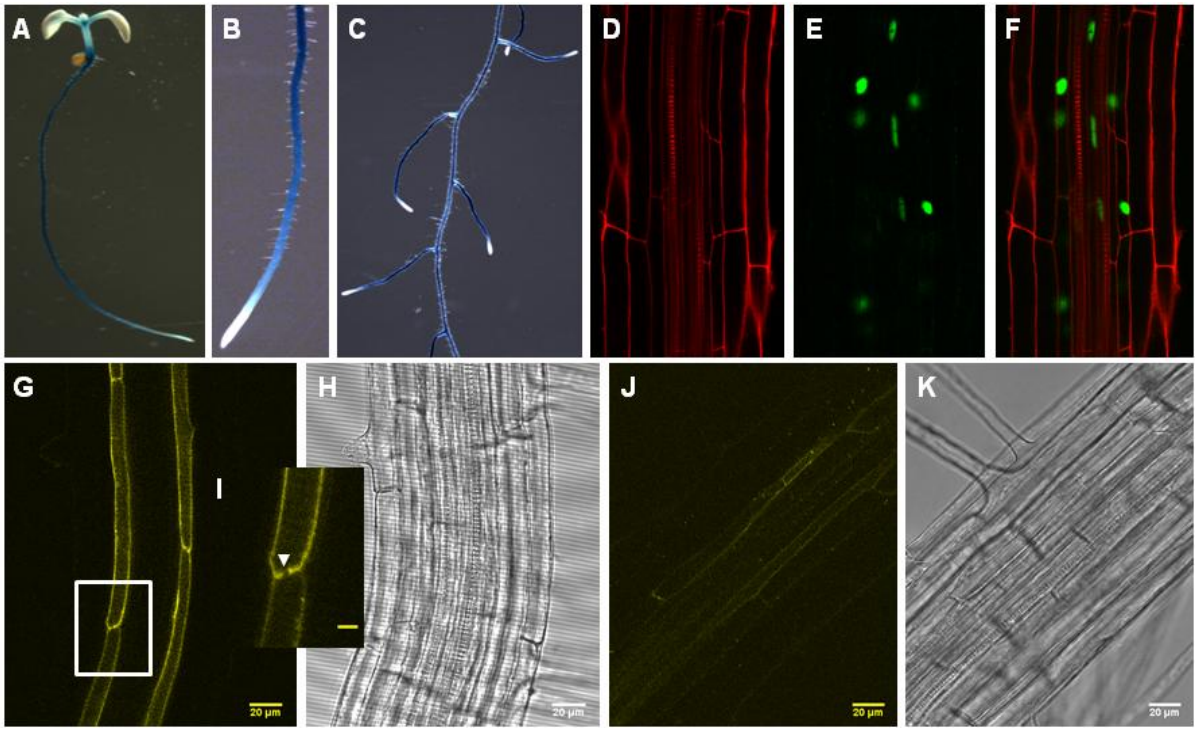

Figure 1

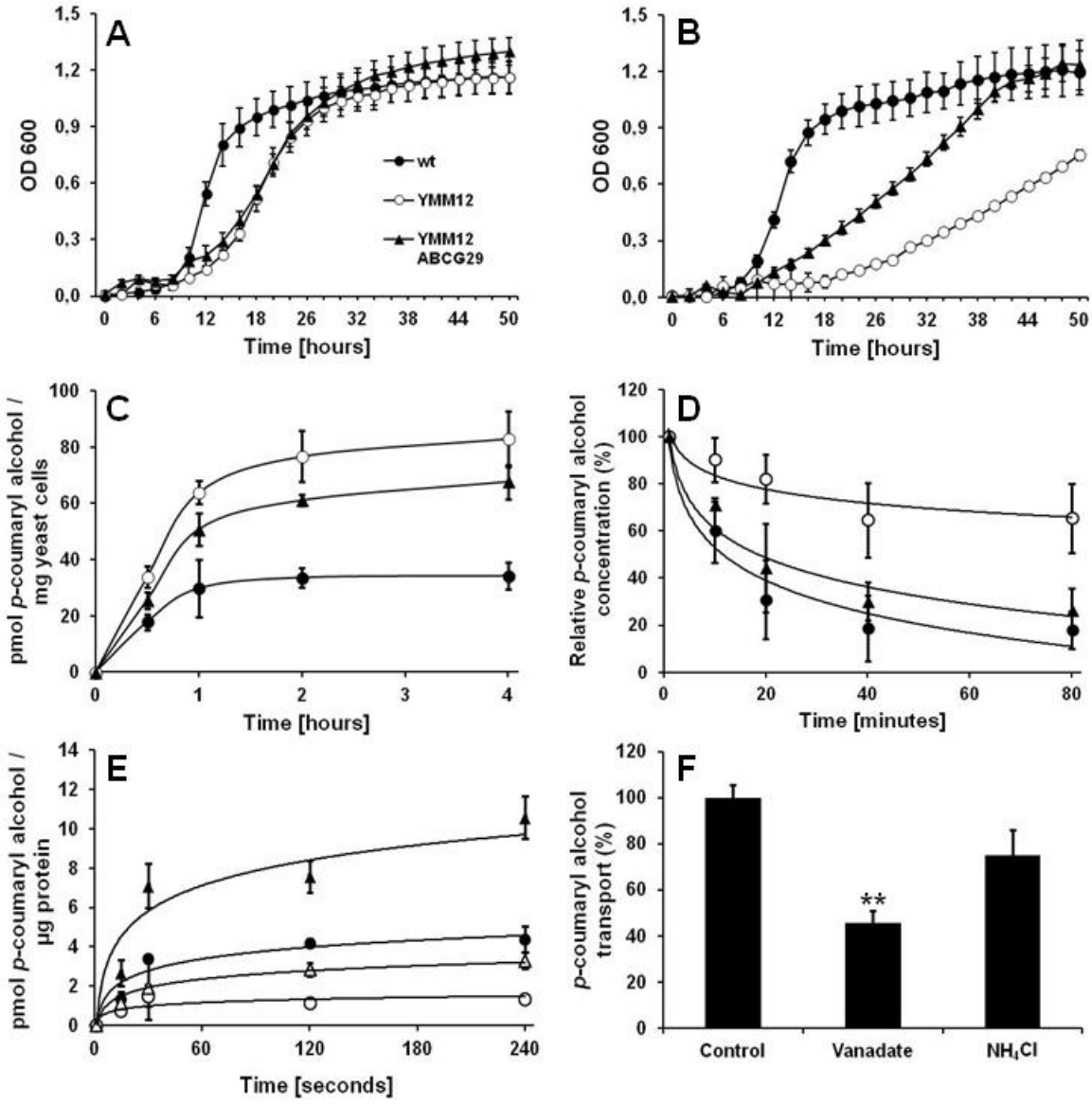
A
OD 600
Time [hours]
wt
YMM12
YMM12 ABCG29
B
OD 600
Time [hours]
C
pmol p-coumaryl alcohol / mg yeast cells
Time [hours]
D
Relative p-coumaryl alcohol concentration (%)
Time [minutes]
E
pmol p-coumaryl alcohol / µg protein
Time [seconds]
F
p-coumaryl alcohol transport (%)
**
Control
Vanadate
NH4Cl

Figure 2

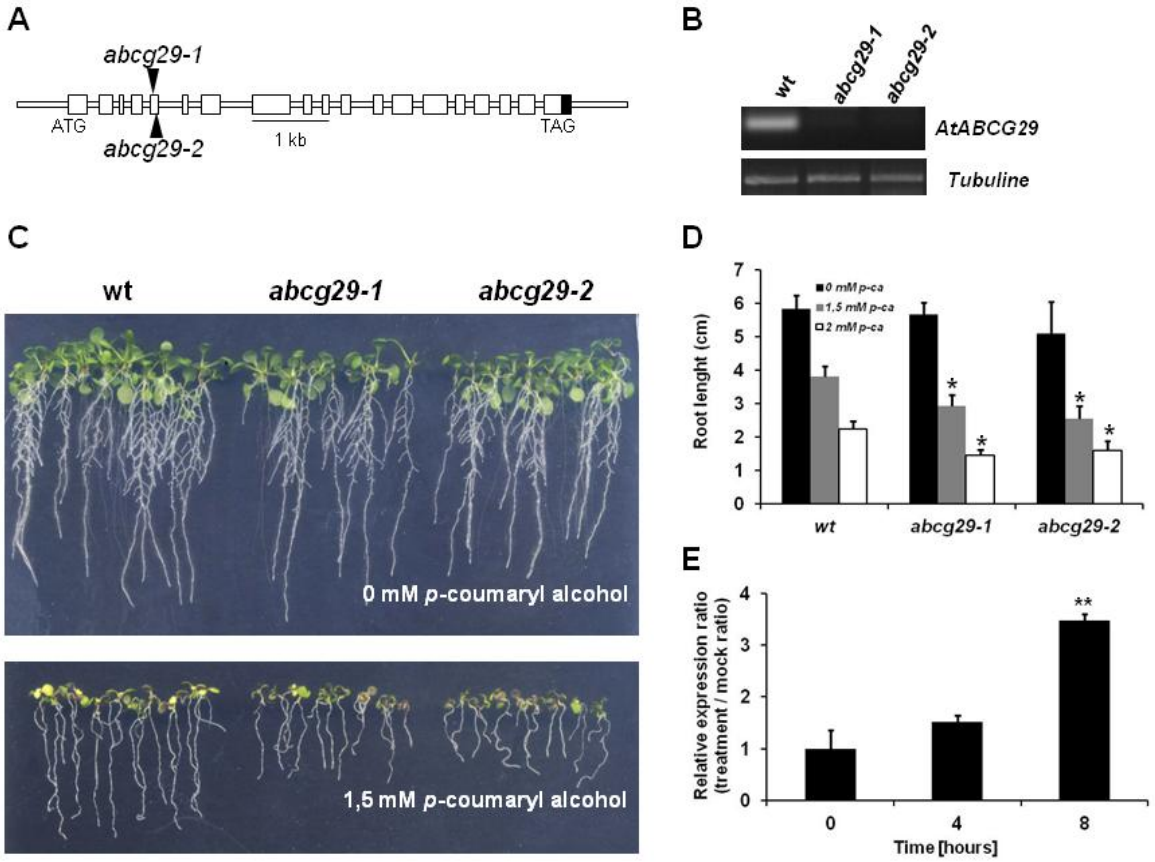
A
abcg29-1
ATG
abcg29-2
1 kb
TAG
B
wt
abcg29-1
abcg29-2
AtABCG29
Tubuline
C
wt
abcg29-1
abcg29-2
0 mM p-coumaryl alcohol
1,5 mM p-coumaryl alcohol
D
0 mM p-ca
1,5 mM p-ca
2 mM p-ca
Root lenght (cm)
wt
abcg29-1
abcg29-2
E
Relative expression ratio (treatment / mock ratio)
Time [hours]

Figure 3

TABLE I. Changes in the contents of lignin hydrolysis products in *abcg29* mutant lines, as identified by GC-MS and thioacidolysis. Data are presented as nmol/g F.W.. Relative peak areas of erytho- and threo- forms are summarised and used for evaluation of unit levels of *p*-hydroxyphenyl (H), guaiacyl (G) and syringyl (S) forms, respectively. Analysis was conducted with four independent biological replicates. SE= Standard error. * $p<0.05$ ** $p<0.01$

	wt (SE)	*abcg29-1* (SE)	*abcg29-2* (SE)
p-hydroxyphenyl (H)	11.0 (± 0.6)	7.7 (± 1.0)*	8.5 (± 0.3)**
guaiacyl (G)	112.9 (± 4.5)	85.9 (± 9.8)*	87.7 (± 1.3)**
syringyl (S)	5.6 (± 0.6)	3.8 (± 0.5)*	3.9 (± 0.3)*

Supplemental Experimental Procedures

Heterologous expression of AtABCG29 and transport assays

S. cerevisiae strains used in this study were: wild type YPH499 (*MATa; ade2-201; his3-200; leu2-1; ura3-52; trp1-63; lys2-801*) and the mutant YMM12 (Δ*snq2::hisG; Δpdr10::hisG; Δpdr12::hisG; Δpdr5::TRP1; Δpdr15loxP-KanMx-lox; Δpdr18::hisG; Δpdr11::HIS3-MX6; Δyor1::HIS3-MX6*). *AtABCG29* was cloned into *Not*I site of pNEV vector. For continuous growth experiments, yeast strains were grown in microtiter plates in a fluorimeter Fusion-α (Packard). Yeast cultures were grown in minimal glucose medium (SCD), and harvested by centrifugation at midlog phase. They were washed twice using SCD medium, and they were resuspended in the same medium. Monolignols were then added to the cell suspension and gently mixed. At the times indicated, the cell suspension was pellet by centrifugation, and the cells were washed with 500 µl of ice-cold water. Cells were broken by glass beads and the monolignol content was determined by HPLC.

Yeast microsomes

The YMM12 yeast mutant was transformed with the expression vector pNEV harboring no insert (YMM12) or *AtABCG29* cDNA (YMM12 ABCG29). Microsomal vesicles were isolated as described previously [28]. *p*-coumaryl alcohol was added to the reaction mix consisting of transport buffer, 1 mM dithiothreitol, 5 mM ATP, 10 mM $MgCl_2$, 10mM creatine phosphate, and 100 µg/ml creatine kinase. Yeast microsomes were added to start the transport assay. The assays were performed at room temperature. At intervals, *p*-coumaryl alcohol uptake was terminated by the transfer of three aliquots onto 0.45 µm-diameter pore size nitrocellulose filters and extracted

with 0.5 ml of methanol-water (1:1 v/v). The supernatant was dried, and samples were resuspended with water. *p*-coumaryl alcohol content was determined by HPLC.

Analysis of soluble monolignols

Monolignols in the aqueous phase were quantified by reversed-phase HPLC using a Hypersil column (MZ Analytical) (5 mm, 250 x 4.6 mm) with gradient elution by an HPLC Dionex system, employing an increasing gradient of methanol-acetonitrile (25:75, v/v) acidified with 0.1% trifluoroacetic acid (solvent B) in 0.1% aqueous trifluoroacetic acid (solvent A). The following gradient elution conditions were used: time= 0 min/0% B; time= 25 min/60% B; time= 27 min/100% B; flow rate= 1.5 ml/min; temperature 40 °C; injection loop= 150 µl. All solvents were of HPLC grade purity. Absorbance spectra were recorded with a Dionex PDA-100 photodiode array detector by scanning from 200 to 450 nm. The peak height was quantified at the maximum absorbance value between 230 and 450 nm. Data collection and integration was performed using the Chromeleon software.

AtABCG29 localization

For construction of *pABCG29::NLS-GFP-GUS*, 2.2 kb of the *AtABCG29* promoter was amplified using genomic DNA from *A. thaliana* as template and the primers pPDR1-attB1 (5'-GGGGACAACTTTGTATAGAAAAGTTGCTGTATGTTCCTATTGGA TAAGGGCATCTTG-3') and pPDR1-attB1r (5'-GGGGACTGCTTTTTTGTACAAACT TGCTTTTTTTTTTTTTGGTGGATTTGGGAA-3'). To determine the subcellular location of AtABCG29, a citrine protein was fused to the N-terminus of *AtABCG29* (*Citrine-ABCG29*). To generate the fusion construct, 1,7 kb genomic fragment of *AtABCG29* was amplified by PCR with PDR1-gDNA Sense (5'-GACATTGTTCA TGGATGAGATATCGACAG-3') and PDR1-gDNA AS (5'-GTTAAAGAGAACCGTAA

ACCCGAGAATGC-3'). The PCR products were cloned using a Multisite Gateway System (Invitrogen). The constructs were introduced into the *Agrobacterium tumefaciens* GV3101 strain, which was then used to transform *A. thaliana* (Col-0) by the dipping method. Confocal laser scanning microscopy was performed on an inverted Leica TCS SP2 AOBS confocal microscope.

Metabolite analysis by *Gas Chromatography Mass Spectrometry* (GC-MS)

Metabolite analysis by GC-MS was carried out essentially as described in [29]. Ground frozen *Arabidopsis* root tissue (50 mg) was homogenized using a ball mill precooled with liquid nitrogen and extracted in 1400 µl of methanol, and 60 µl of internal standard (0.2 mg ribitol ml^{-1} water) was subsequently added as a quantification standard. Chromatogram and mass spectra were evaluated using either TaGFinder [30] or the MASSLAB program (ThermoQuest), and the resulting data were prepared and presented as described in [31]. The mass spectra were cross-referenced with those in the Golm Metabolome Database [32]. Analysis was conducted with three independent biological replicates.

Metabolite analysis by *Liquid Chromatography Mass Spectrometry* (LC-MS)

Ground frozen roots were aliquoted and homogenized in 5 µl of extraction buffer (80% MeOH, 10µg ml^{-1} isovitexin) per milligram of fresh weight of tissue in a mixer mill for 3 min at 25 Hz with gilconia ball. After centrifugation at 12,000*g*, the supernatants were immediately used for general secondary metabolite analysis. General secondary metabolite analysis by LC-MS was performed on HPLC system Surveyor (Thermo Finnigan, USA) coupled to Finnigan LTQ-XP system (Thermo Finnigan, USA) as described in [33]. All data were processed using Xcalibur 2.1 software (Thermo Fisher Scientific, Waltham, USA). The obtained data matrix was normalized using the internal standard (isovitexin, CAS: 29702-25-8). Metabolite

identification and annotation were performed using standard compounds [24] and previous work [34,35]. Analysis was conducted with three independent biological replicates.

Cell wall purification

Isolation of cell wall fraction was performed according to the method described in [36]. Five hundred mg of grounded frozen root materials were homogenized in a mixer mill for 3 min at 25 Hz with gilconia ball in 50% MeOH (1 ml). The supernatant was removed and the residues were washed sequentially with the following solutions: MeOH, H_2O, 0.5% SDS, 1 M NaCl, H_2O, MeOH, Me_2CO and *n*-hexane (2×1 ml each, shaken and centrifuged as above). The residues were operationally defined as purified cell walls and stored at −20 °C after drying by a Speed-Vac (Eppendorf, Hamburg, Germany).

GC-MS analysis of lignin thioacidolysis products

Derivatisation followed by thioacidolysis cleavage is a method for lignin compositional analysis that produces analyzable monomers by cleaving ethers in lignin [18,19]. Dried cell wall fractions (prepared from 500 mg F.W. of roots sample) were transferred to glass vials with a Teflon-lined screw-cap, and suspended in 3 ml of reaction mixture (0.2M boron trifluoride etherate in dioxane/ethantiol (8.75/1, v/v) with nitrogen gas). Reaction mixtures were gently stirred in an oil bath at 100°C for 4.0 h. After being cooled in ice, the thioacidolytic products were poured into dichloromethane (3 ml) and added 3 ml of distilled water. The pH of aqueous phase was adjusted with sodium bicarbonate (0.4M) to 4.0. The organic phase was extracted using dichloromethane (3 ml x 2) and evaporated to dryness completely. The residues were dissolved in dichloromethane (500 µl). After centrifugation at

12,000*g*, 100 µl of supernatant was evaporated and injected to GC-MS analysis which was a method as described previously with TMS derivatisation step [29]. Detected ethanethiolated phenyl alcohols were identified by their trimethylsilylated standard compounds (*p*-coumaryl alcohol, coniferyl alcohol and sinapyl alcohol). Relative peak areas of *erytho*- and *threo*- forms are summarized and used for evaluation of unit levels of *p*-hydroxyphenyl (H), guaiacyl (G) and syringyl (S) forms, respectively. Analysis was conducted with four independent biological replicates.

Supplemental References

29. Tommasini, R., Evers, R., Vogt, E., Mornet, C., Zaman, GJ., Schinkel, AH., Borst, P., Martinoia, E. (1996). The human multidrug resistance-associated protein functionally complements the yeast cadmium resistance factor 1. Proc. Natl. Acad. Sci. 93, 6743–6748

30. Lisec, J., Schauer, N., Kopka, J., Willmitzer, L. and Fernie, AR. (2006) Gas chromatography mass spectrometry-based metabolite profiling in plants. Nat Protoc, 1, 387-396.

31. Luedemann, A., Strassburg, K., Erban, A. and Kopka, J. (2008) TagFinder for the quantitative analysis of gas chromatography--mass spectrometry (GC-MS)-based metabolite profiling experiments. Bioinformatics, 24.

32. Roessner, U., Willmitzer, L. and Fernie, AR. (2001) High-resolution metabolic phenotyping of genetically and environmentally diverse potato tuber systems. Identification of phenocopies. Plant Physiology, 127, 749-764.

33. Kopka, J., Schauer, N., Krueger, S., Birkemeyer, C., Usadel, B., Bergmuller, E., Dormann, P., Weckwerth, W., Gibon, Y., Stitt, M., Willmitzer, L., Fernie, AR. and Steinhauser, D. (2005) GMD@CSB.DB: the Golm Metabolome Database. Bioinformatics, 21, 1635-1638.

34. Tohge, T. and Fernie, AR. (2010) Combining genetic diversity, informatics and metabolomics to facilitate annotation of plant gene function. Nature Protocols, 5, 1210-1227.

35. Nakabayashi, R., Kusano, M., Kobayashi, M., Tohge, T., Yonekura-Sakakibara, K., Kogure, N., Yamazaki, M., Kitajima, M., Saito, K. and Takayama, H. (2009)

Metabolomics-oriented isolation and structure elucidation of 37 compounds including two anthocyanins from Arabidopsis thaliana. Phytochemistry, 70, 1017-1029.

36. Tohge, T., Nishiyama, Y., Hirai, MY., Yano, M., Nakajima, J., Awazuhara, M., Inoue, E., Takahashi, H., Goodenowe, DB., Kitayama, M., Noji, M., Yamazaki, M. and Saito, K. (2005) Functional genomics by integrated analysis of metabolome and transcriptome of Arabidopsis plants over-expressing an MYB transcription factor. Plant J., 42, 218-235.

37. Tan, J.W., Bednarek, P., Liu, H.K., Schneider, B., Svatos, A. and Hahlbrock, K. (2004) Universally occurring phenylpropanoid and species-specific indolic metabolites in infected and uninfected Arabidopsis thaliana roots and leaves. Phytochemistry, 65, 691-699.

Supplemental Figure S1. Co-expression gene network around ABCG29. Coexpression network analyses were carried out using NetworkDrawer (http://atted.jp/top_draw.shtml#NetworkDrawer) on the coexpression gene search program ATTEDII ver.6.0. Coexpression network was constructed with ABCG29 (At3g16340) and well-correlated genes with ABCG29 (4-coumarate coenzyme A ligase 2, 4CL2, At3g21240; 4CL5, At3g21230; caffeoyl coenzyme A *O*-methyltransferase 1, CCoAMT1, At4g34050; respiratory burst oxidase protein, RBOHF At1g64060). Common biochemical pathways in the network are denoted by color-coded dots within the nodes.

Supplemental Figure S2. AtABCG29 GUS staining. Expression pattern of AtABCG29 using a *AtABCG29* promoter-GUS (*promABCG29::NLS-GFP-GUS*) construct in roots of 2-week-old plant (**A**), stem and rosette leaves 2-3 weeks after bolting (**B**), anther (**C**) and silique (**D**) gene expression.

Supplemental Figure S3. Growth in coniferyl and sinapyl alcohol of a mutant in ABC transporters and sinapyl alcohol uptake in yeast microsomes. The growth of the indicated wild type yeast (YPH449, wt, black circles), mutant strain with the empty pNEV vector (YMM12, open cicles) and *AtABCG29* overexpression (YMM12 ABCG29, black triangles) was monitored. The yeast cells were grown in SCD + 2mM coniferyl alcohol (**A**) or SCD + 3mM sinapyl alcohol **(B**). The growth curves are derived from the mean values of four independent cultures for each time point. The experiment was repeated three times with similar results. (**C**) Time-dependent sinapyl alcohol uptake into microsomes from yeast cells containing either the empty vector or expressing AtABCG29. Open circle, pNEV -ATP; filled circle, pNEV +ATP;

open triangle, pNEV-AtABCG29 -ATP; filled triangle, pNEV-AtABCG29 +ATP. Results are the mean values of three independent cultures for each time point. The experiment was repeated three times with similar results.

Supplemental Figure S4. Heat map visualization of relative differences in metabolite pools between wt and *abcg29* mutant lines and transcription level of genes coding enzymes of phenylpropanoid and glucosinolates biosynthesis pathway. Metabolites detected by (**A**) GC-MS analysis and (**B**) LC-MS analysis. Both data were obtained from 3-week-old roots grown on agar plates. Log_2 Fold Change (Log_2FC) were estimated by setting the wild type=0. Abbreviations: Q-3GR-7R, quercetin-3-*O*-(2″-*O*-Rha)Glc-7-*O*-Rha; K-3GR-7R, kaempferol-3-*O*-(2″-*O*-Rha)Glc-7-*O*-Rha; K-3G-7R, kaempferol-3-*O*-Glc-7-*O*-Rha; K-3R-7R, kaempferol-3-*O*-Rha-7-*O*-Rha; A9, Cyanidin 3-*O*-[2″-*O*-(2‴-*O*-(Sin)Xyl 6″-*O*-(*p*-*O*-Cou)Glc] 5-*O*-[6⁗-*O*-(Mal)Glc]; Sinapoyl-Mal, sinapoyl-malate; 3MSOP, 3-methylsulfinylpropyl glucosinolate; 4MSOB, 4-methylsulfinylbutyl glucosinolate; 8MSOO, 8-methylsulfinyloctyl glucosinolate; 4MTB, 4-methylthiobutyl glucosinolate; 5MSP, 5-methylthiopentyl glucosinolate; I3M, 4-hydroxy-indolyl-3-methyl glucosinolate; 1MOI3M,1-methoxy-indolyl-3-methyl glucosinolate; 4MOI3M, 4-methoxy-indolyl-3-methyl glucosinolate. (**C**) Relative transcript levels of genes involved in phenylpropanoid and glucosinolates biosynthesis pathway. RNA was extracted from roots of 3-week-old seedlings grown in agar plates. RNA extraction a qRT-PCR was made as described in figure 4. Results are the mean values of three independent cultures. The experiment was repeated three times with similar results. * p <0,05. *4CL2* (4-coumarate CoA ligase 2), *ASB1* (anthranilate synthase beta subunit 1), *CHS* (chalcone synthase), *CM1* (chorismate mutase 1) and *PAL1* (phenylammonia lyase 1). The primer sets for the analyzed genes were as follows: 5'-

GGTAAGGAGCTTGAAGATGC-3’ (F) and 5’-CTCTTTACGAAACCCTAACG-3’ (R) for *4CL2*; 5’-GCAGCATGGTCCAATCATCG-3’ (F) and 5’-TCATCATTGCGGTAAACTTC-3’ (R) for *ASB1*; 5’-CAGTGAACACATGACCGACC-3’ (F) and 5’-ATGTCCTGTCTGGTGTCCAG-3’ (R) for *CHS*; 5’-TCACGCCGTTATGACACTCG-3’ (F) and 5’-TGTAACAGTACTTGGCTCTC-3’ for *CM1*; 5’-TCA TCGGAGAACCAAAAACG-3’ (F) and 5’-GCTATGGGTGTGAACCAACC-3’ (R) for *PAL1*; 5’-CCTGATAACTTCGTCTTTGG-3’ (F) and 5’-GTGAACTCCATCTCGTCCAT-3’ for *Tubuline*.

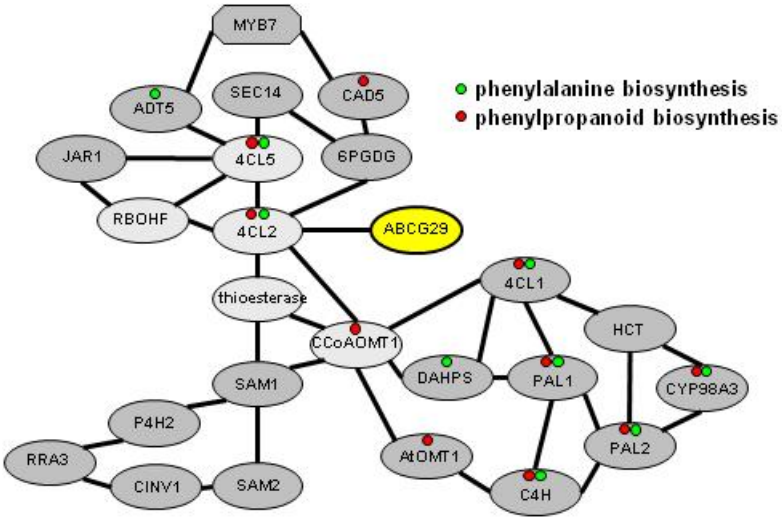

Supplemental Figure S1

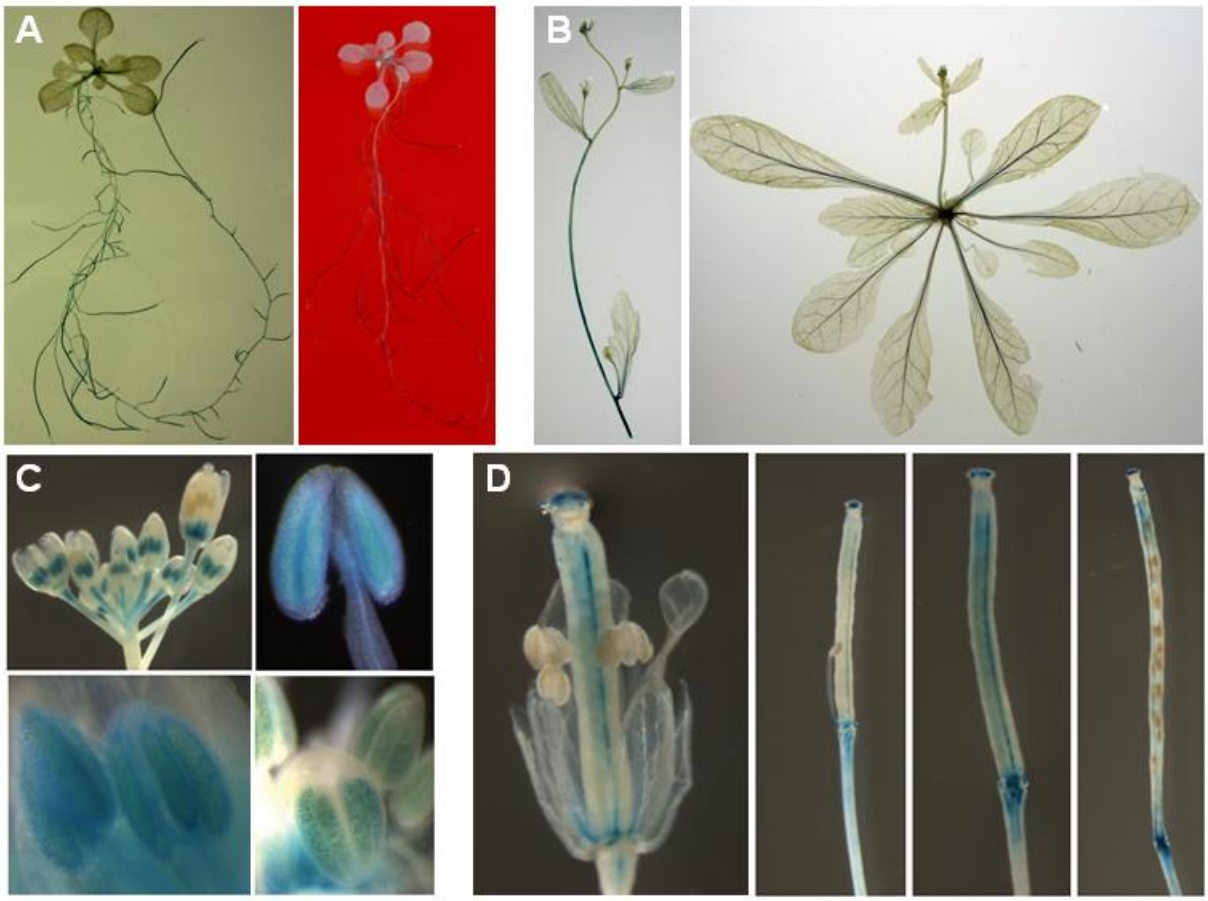

Supplemental Figure S2

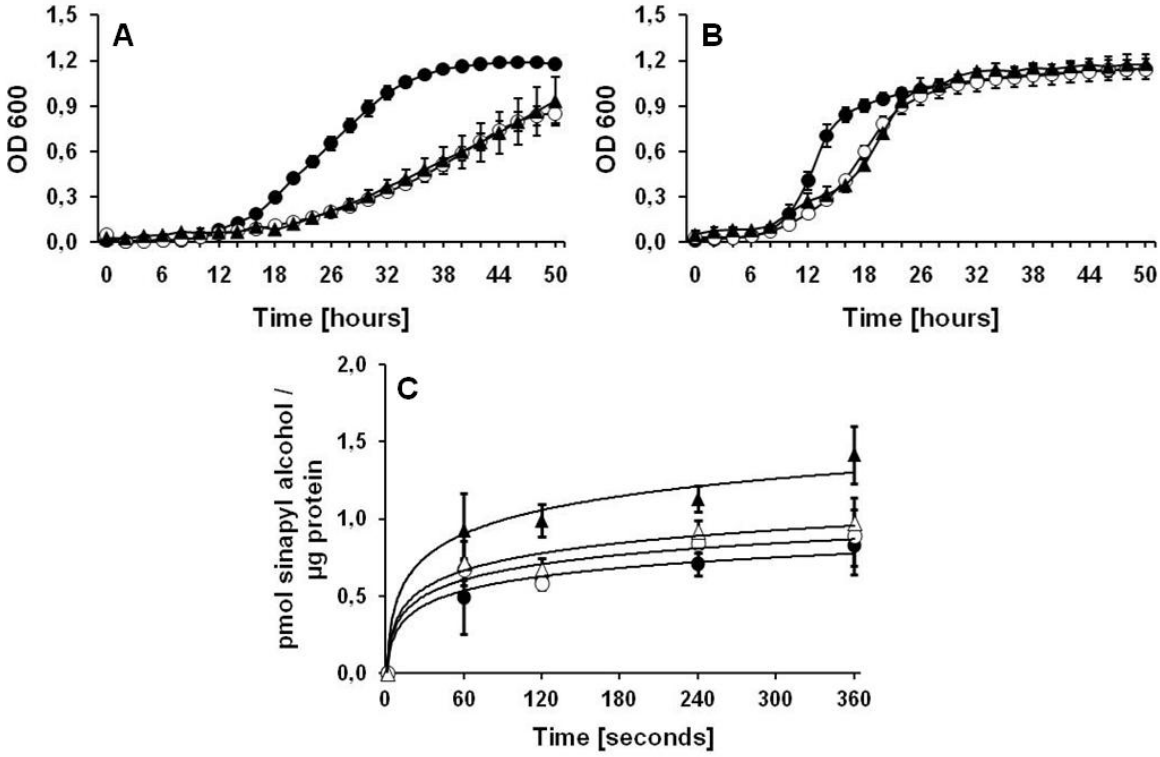

Supplemental Figure S3

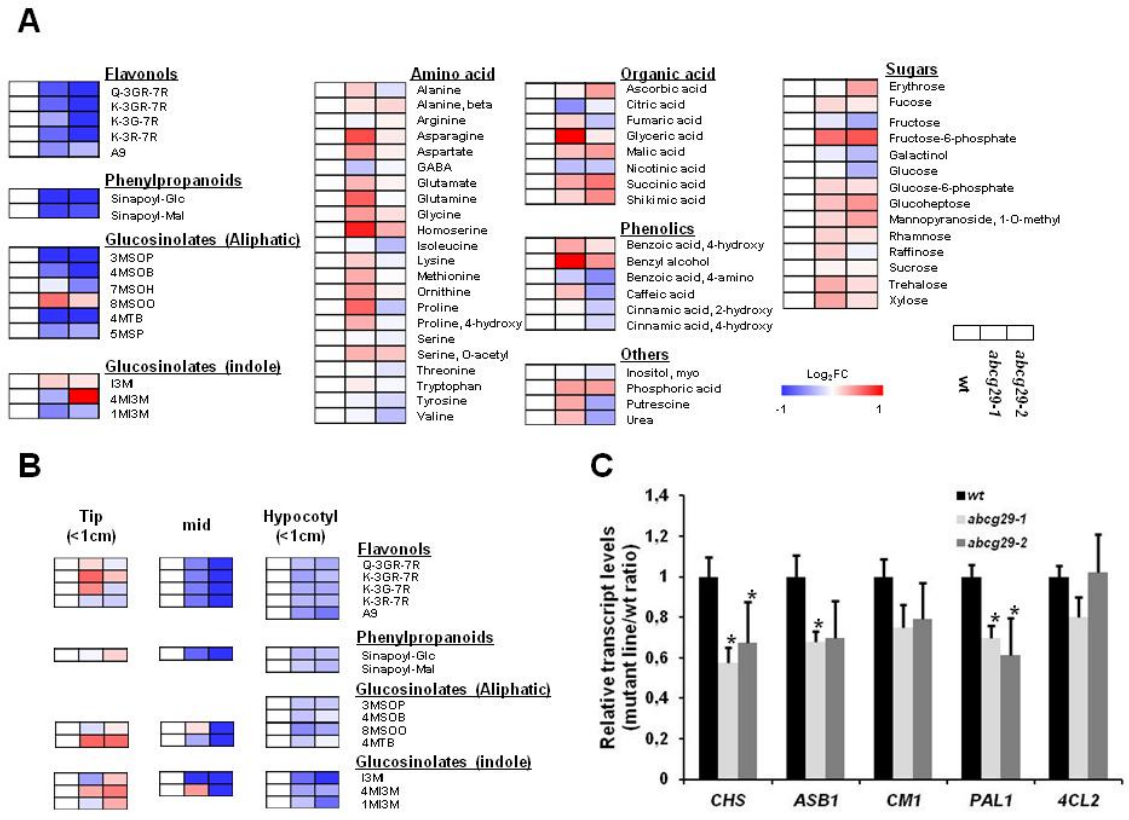

Supplemental Figure S4